Complementary human gene interaction maps from radiation hybrids and CRISPRi

Desmond J. Smith[1,*]

[1] *Department of Molecular and Medical Pharmacology, David Geffen School of Medicine, UCLA, Los Angeles, USA*
[*] *DSmith@mednet.ucla.edu*

The only comprehensive genetic interaction map of the human genome was constructed using increased gene copy number in radiation hybrid (RH) cells. More recently, interactions restricted to essential genes were identified using loss-of-function alleles made by CRISPRi technology. I compared the two maps to understand their similarities and differences. Both maps overlapped significantly with a database of protein-protein interactions. However, interactions in the RH and CRISPRi datasets had no significant overlap, even though the participating genes overlapped significantly. In addition, the RH map showed highly significant similarity with an interaction map constructed from genome-wide association studies (GWASs), while the CRISPRi map did not. This study reveals that gain- and loss-of-function alleles highlight different aspects of the genetic interaction landscape.

Introduction

Comprehensive genetic interaction maps of the human genome have been daunting to construct because of the large number of potential interactions. For the ~20 000 protein coding genes, there are $\sim 2.0 \times 10^8$ potential interactions.[1] The inclusion of non-coding transcripts trebles the number of genes, increasing the potential number of interactions to $\sim 1.8 \times 10^9$.

Radiation hybrid (RH) mapping emerged in the 1990s as a statistical approach to high resolution mapping of the human genome.[2,3] Human cells are lethally irradiated, fragmenting the DNA. A random sample of the fragments are then transferred to living cells using cell fusion (**Figure 1A**).

The small size of the fragments allows construction of high resolution genetic maps. Markers that lay close to each other in the genome tend to be coinherited in the RH clones.

Usually distant genes are inherited independently. However, genes that interact will show coinheritance even if at a distance in the genome.[4] For example, the poisonous effect of an extra gene copy on cell growth may be "blocked" by an extra copy of a distant gene. These two genes will show significant coinheritance in the RH clones, and constitute an "attractive" interaction.

In contrast, two distant genes that together inhibit cell proliferation will show significant non-coinheritance, a "repulsive" interaction.

Each RH clone harbors ~10-25% of the genome as an extra copy. This high degree of multiplexing gives the technique extraordinary efficiency and allows it to evaluate interactions for the entire genome, a prospect out of reach for approaches that evaluate gene pairs one-at-a-time in each cell.

We used the RH approach to construct an interaction network for the entire human genome, including coding and non-coding genes.[4] PCR genotyping data of 560 RH clones from human, mouse, rat and dog were employed, using the human genome as a scaffold.

In contrast to the extra gene copies used in the RH networks, CRISPR interference (CRISPRi) evaluates interactions using partial loss-of-function (hypomorphic) alleles.[5] CRISPRi targets genes by employing a catalyt-

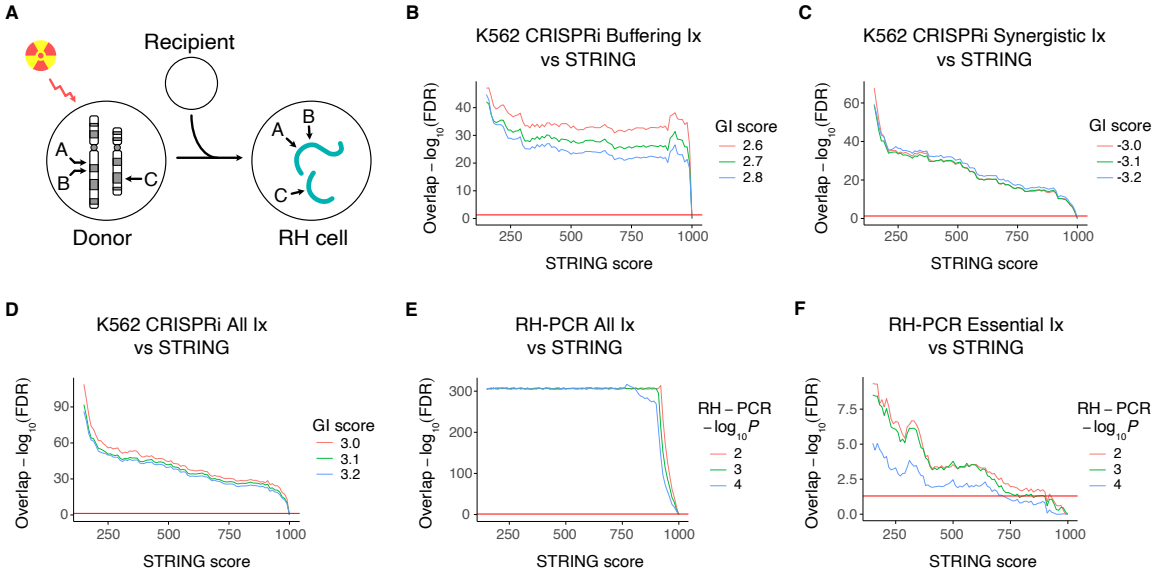

Figure 1. RH-PCR, CRISPRi and STRING interaction networks. (**A**) Construction of RH cells. Genes A and B lay close to each other in the genome and tend to be co-inherited in the RH cells. Gene C is a long way from A and B, and is inherited independently unless it interacts with either A or B. Small DNA fragments, torquoise strands. Recipient cell chromosomes not shown. (**B**) Overlap of K562 buffering CRISPRi interactions and STRING. The higher the STRING score threshold, the greater the confidence in the protein-protein interaction. GI, CRISPRi genetic interaction. Positive GI scores, buffering interactions; negative, synergistic. Horizontal red line, FDR = 0.05. (**C**) Overlap of K562 synergistic CRISPRi interactions and STRING. (**D**) Overlap of K562 combined buffering and synergistic CRISPRi interactions and STRING. (**E**) Overlap of protein coding RH-PCR network and STRING. (**F**) Overlap of RH-PCR interactions restricted to essential genes in the CRISPRi dataset and STRING.

ically inactive version of Cas9 fused to a transcriptional repressor.

The CRISPRi technology only targets one gene pair in each cell, limiting throughput and investigative scope. Recently, CRISPRi was used to catalog interactions among essential protein coding genes selected to have a moderate individual loss-of-function growth phenotype in K562 and Jurkat cells.[5]

The CRISPRi network assessed ∼0.05 % of all potential protein coding interactions, in contrast to the RH-PCR network which examined the entire genome.

The CRISPRi study identified two types of interaction. Buffering interactions (traditionally called epistatic) occurred when the combination of two loss-of-function alleles resulted in better cell growth than either alone. In contrast, synergistic interactions occurred when the combination of alleles resulted in poorer cell growth than either alone.

In this study, the RH-PCR and CRISPRi interaction maps are used to compare and contrast the biological effects of extra gene copies and partial loss-of-function alleles. In particular, the similarities of the genetic interaction maps with protein-protein interaction networks are examined. Overlaps with interaction maps obtained using genome-wide association studies (GWASs) are also evaluated.

Results

Properties of RH-PCR and CRISPRi networks

The full RH-PCR network consisted of 7 248 479 significant interactions featuring 18 220 genes (false discovery rate, FDR < 0.05).[4,6] When restricted to protein coding genes, the RH-PCR network had 2 705 945 interactions among 10 897 genes. Of these interactions, 912 (0.03 %) were repulsive and the remainder attractive. None of the genes involved in repulsive interactions were in the CRISPRi dataset.

Interaction strengths in the CRISPRi networks were quantitated using a genetic interaction (GI) score, with positive GI scores indicating buffering interactions and negative indicating synergistic.[5] The greater the magnitude of the GI score, the greater the interaction strength. Significant GI thresholds based on negative controls in K562 cells were > 2.5 and < -2.6, for buffering and synergistic interactions respectively, and > 1.9 and < -2.0 for Jurkat (**Materials and Methods**).

Using CRISPRi, a total of 100 128 potential interactions among 448 essential genes were tested in K562 cells. Of the tested interactions, 3885 (3.9 %) had significant growth effects and featured 446 genes.

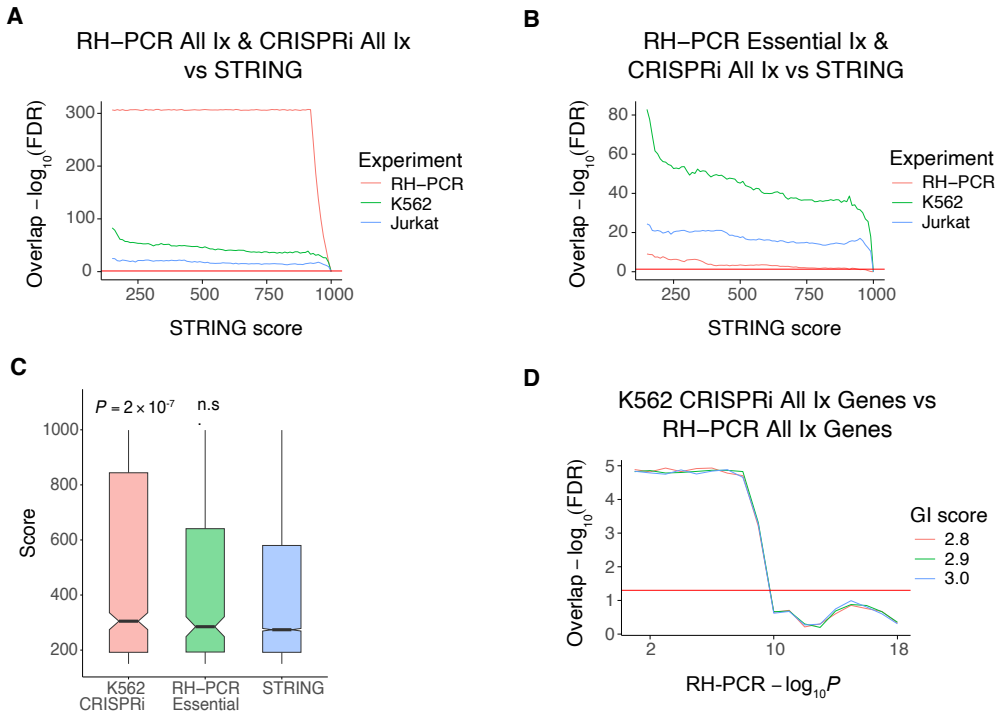

Figure 2. Overlaps of genetic interaction networks and their participating genes. (**A**) Overlaps of protein coding RH-PCR and K562 and Jurkat combined buffering and synergistic CRISPRi interactions with STRING. (**B**) Overlaps of essential RH-PCR and K562 and Jurkat combined CRISPRi networks with STRING. (**C**) STRING scores for interactions specific to K562 combined CRISPRi, essential RH-PCR and STRING networks. (**D**) Overlaps of genes involved in interactions in K562 combined CRISPRi and protein coding RH-PCR networks.

Of these interactions, 1493 were buffering and 2392 synergistic.

In Jurkat cells, a total of 95 266 interactions were tested using 436 essential genes. A total of 2552 (2.7 %) interactions featuring 424 genes had significant growth effects. Of the interactions, 1318 were buffering and 1234 synergistic.

The protein coding RH-PCR network contained ∼840 times more significant interactions than the CRISPRi network and ∼25 times more genes.

Network subsets

Three subsets of the full RH-PCR network were used in network comparisons.

(1) The protein coding RH-PCR network ("All").
(2) The protein coding RH-PCR network restricted to the essential genes evaluated in the CRISPRi study (279 genes, 1778 interactions for K562; 273 genes, 1686 interactions for Jurkat). The "essential" RH-PCR network allowed equally powered overlap comparisons with the CRISPRi networks.
(3) Essential RH-PCR network plus genes linked by one interaction (10 497 genes, 140 308 interactions for K562; 10 497 genes, 140 216 interactions for Jurkat). The "essential plus one" RH-PCR network is intermediate in size between first two subsets.

Similarly, three subsets of the CRISPRi networks were used.

(1) Buffering, with significant positive GI scores.
(2) Synergistic, with significant negative GI scores.
(3) Combined, with all significant GI scores regardless of sign.

In network comparisons using the CRISPRi data, statistics from K562 cells are reported. Observations from the Jurkat cells are presented in the **Supplmental Information**, and were essentially similar.

Overlap significance

The overlap significance of two genetic interaction networks depends on the thresholds used to define the interactions in each of them. Rather than simply using one threshold, I surveyed the whole overlap terrain by scanning threshold parameters from least to most stringent.[7] The overlap significance at each threshold was then calculated, correcting for multiple tests using false discovery rates.[6]

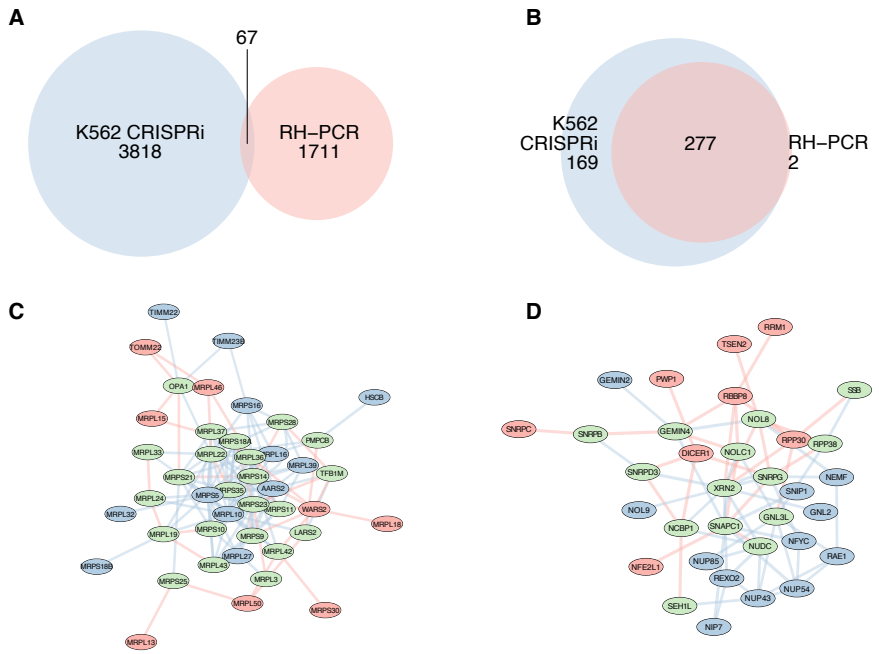

Figure 3. Overlaps of interactions and genes. (**A**) Overlap of interactions in the essential RH-PCR and K562 combined buffering and synergistic CRISPRi networks. (**B**) Overlap of genes involved in interactions in the two networks. (**C**) Interactions between mitochondrial genes in essential RH-PCR and K562 combined CRISPRi networks. Red nodes and edges, RH-PCR network only; blue nodes and edges, CRISPRi only; green nodes, both RH-PCR and CRISPRi. Edge width proportional to interaction strength. (**D**) Interactions between genes that encode nuclear-and nucleolus-related proteins in essential RH-PCR and K562 combined CRISPRi networks.

Overlaps of RH-PCR and CRISPRi networks with STRING

First to be examined was the overlap of the protein coding RH-PCR and CRISPRi interaction networks with the STRING database of protein-protein interactions.[8]

STRING v11 contains 5 879 727 human protein-protein interactions, identified by collating information from multiple publicly available sources. Interactions are assigned a score ranging from 150 (lowest confidence) to 999 (highest).

The buffering, synergistic and combined CRISPRi interactions showed significant overlap with STRING in both K562 and Jurkat cells (K562 combined interactions: optimum FDR = 1.3×10^{-109}; odds ratio, OR = 2.9, Fisher's Exact Test) (**Figures 1B-D**, **S1**, **S2**).

The protein coding RH-PCR network also overlapped significantly with STRING (optimum FDR = 4.3×10^{-319}, OR = 1.9) (**Figures 1E**, **S3**), but with greater significance than CRISPRi (**Figures 2A**, **S3**), reflecting the more comprehensive nature of the RH-PCR network.

When restricted to the essential genes evaluated in the CRISPRi study, the RH-PCR interactions still showed significant overlap with STRING (optimum FDR = 4.7×10^{-10}, OR = 1.5) (**Figures 1F**, **S3**), but was less significant than CRISPRi (**Figures 2B**, **S3**).

STRING scores for interactions specific to the K562 or Jurkat CRISPRi network were significantly greater than the null distribution of STRING scores (K562, t[1,1256] = 5.2, $P = 2.3 \times 10^{-7}$; Jurkat, t[1,685] = 4.9, $P = 1.5 \times 10^{-6}$) (**Figure 2C**). In contrast, interactions in the essential RH-PCR network showed no significant difference. The RH-PCR interactions appear to be more representative of protein-protein interactions than the CRISPRi interactions, which preferentially recover interactions in the STRING dataset with higher scores.

Genes involved in RH-PCR and CRISPRi interactions

The essential RH-PCR interaction network did not show significant FDR corrected overlap with the K562 and Jurkat CRISPRi networks. However, there were highly significant overlaps between the genes involved in interactions of the essential RH-PCR and CRISPRi networks (K562 combined interactions: optimum FDR = 1.0×10^{-5}, OR = 1.7) (**Figures 2D**, **S4**, **S5**).

Consistent with these observations, only 67 interactions were common between the 3885 combined buffering and synergistic K562 CRISPRi interactions and 1778 essential RH-PCR interactions (**Figures 3A**, **S6A**). In contrast, of the 446 and 279 genes involved in the K562 CRISPRi and essential RH-PCR interactions,

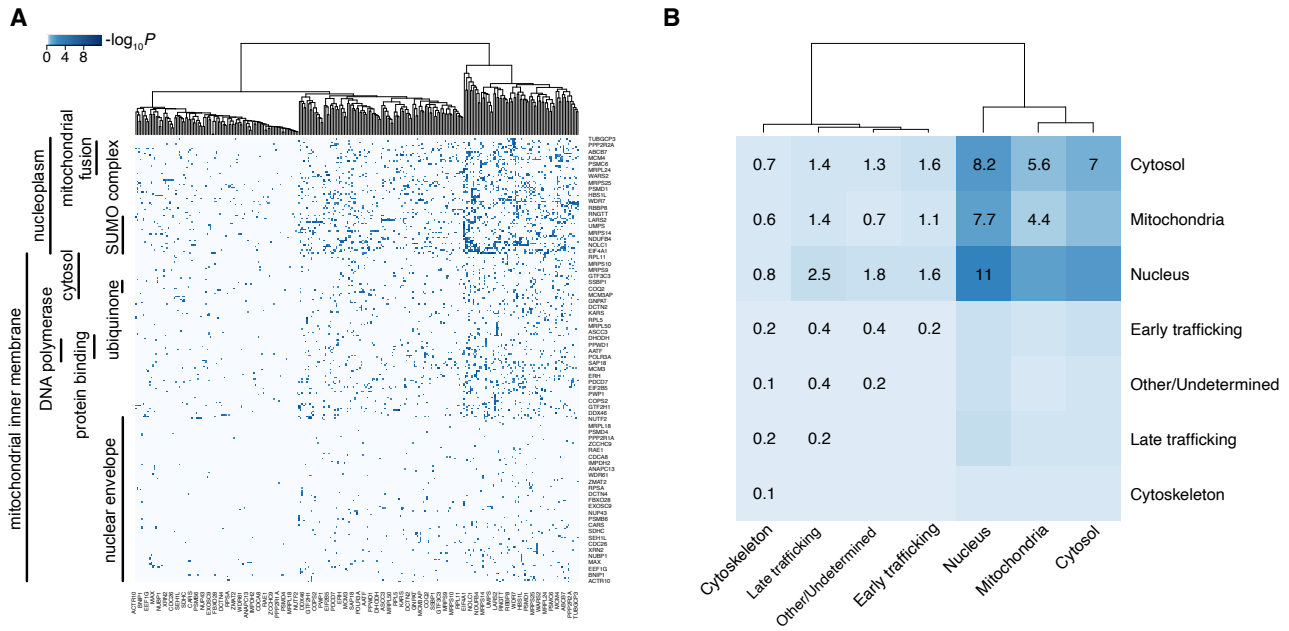

Figure 4. Functional clustering of essential RH-PCR network. (**A**) Clustering of genes based on $-\log_{10}P$ interaction values. Functional enrichments of clusters shown. For reasons of space, only 26 % of the genes in the cluster diagram are labeled. (**B**) Clustering of shared cellular compartments in essential RH-PCR interactions. Percentage of genes in each compartment shown.

respectively, a total of 277 were common (**Figure 3B**, **S6B**). The RH-PCR and CRISPRi approaches identify nearly the same genes involved in genetic interactions, but highlight different sets of interactions among these genes.

Examples of the complementary genetic interactions in the essential RH-PCR and K562 combined CRISPRi networks are shown for mitchondrial and nuclear-related genes in **Figures 3C,D**.

The mitochondrial interaction network obtained by amalgamating the essential RH-PCR and buffering and synergistic K562 CRISPRi datasets involved 43 genes, of which 23 were shared (**Figure 3C**). In contrast, of the 127 interactions in this network only 4 were shared between the essential RH-PCR and CRISPRi networks.

Similarly, the network of essential nuclear- and nucleolus-related genes had 34 genes, of which 14 were shared between the RH-PCR and K562 CRISPRi networks, but of the corresponding 65 interactions only one was shared (**Figure 3D**).

Functional clustering of essential genes in the RH-PCR network

To further explore the essential RH-PCR network, unsupervised clustering of genes based on their interaction $-\log_{10}P$ value was employed (**Figure 4A**). Clusters were then assigned in principled fashion to gene ontology (GO) enrichment categories (FDR $< 10^{-5}$).[9]

Terms relating to mitochondria (mitochondrial inner membrane, mitochondrial fusion), the nucleus (nucleoplasm, nuclear envelope) and cytosol were prominent among the GO enrichments. For example, the mitochondrial inner membrane cluster contains 211 of the 241 genes related to mitochondria in the nuclear genome. Similarly, of the 308 nuclear-related genes in the genome, there were 105 in the nuclear envelope cluster .

Clustering of the CRISPRi interaction network gave similar enrichment patterns, with prominent enrichment of nucleus/cytoplasm, cytosol and mitochondria.[5] However, some GO terms such as mRNA stability and splicing that were prominent in the CRISPRi network did not appear in the essential RH-PCR network.

Cellular compartments of essential genes in the RH-PCR network

Gene interactions are mediated by the locations of the corresponding proteins in the compartments of the cell. To better understand this aspect of the essential RH-PCR network, unsupervised clustering of cellular compartments based on the proportion of interacting genes in each compartment was employed (**Figure 4B**).

Reminscent of the GO enrichment clusters, the 3 compartments with the highest proportion of shared interactions were nucleus, cytosol and mitochondria. The CRISPRi network showed some differences and similarities to the essential RH-PCR network, with strong clustering of mitochondria for buffering interactions

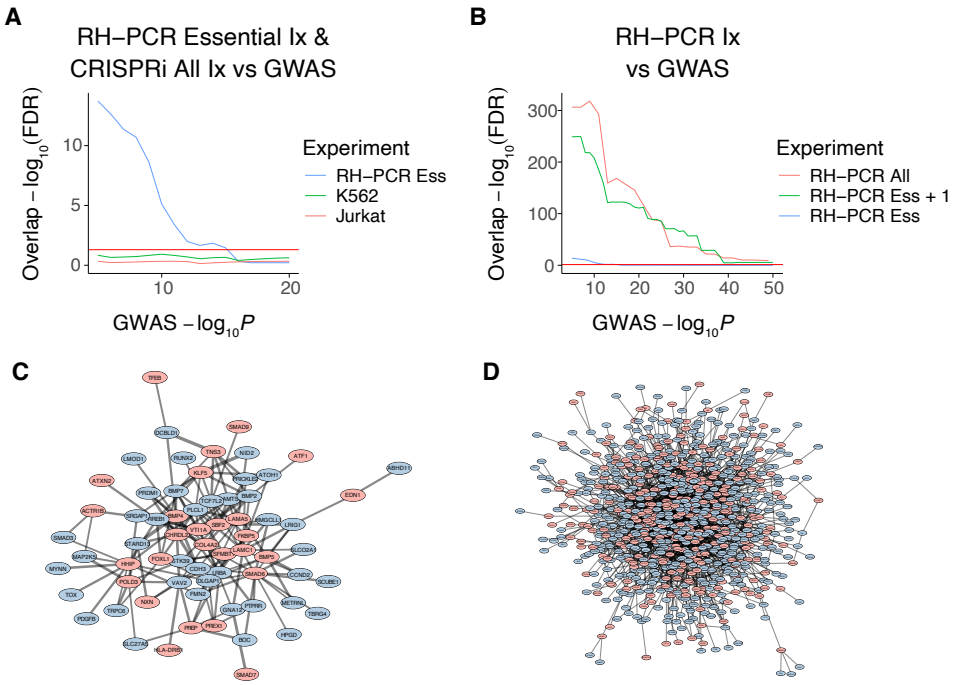

Figure 5. GWAS networks for RH-PCR and CRISPRi interactions. (**A**) Overlaps of essential RH-PCR and K562 and Jurkat combined buffering and synergistic CRISPRi networks with GWAS network. (**B**) Overlaps of full RH-PCR, essential RH-PCR plus genes separated by one link, and essential RH-PCR networks with GWAS network. (**C**) Colorectal GWAS genes from lower power study (blue nodes) and additional genes in the higher power study (pink) predicted by the RH-PCR network. Edge width reflects RH-PCR $-\log_{10}P$. (**D**) Height GWAS.

and other/undetermined and early trafficking for synergistic interactions.[5]

GWAS and genetic interaction networks

The potential of the RH-PCR and CRISPRi networks to cast light on common disease loci from genome-wide association studies (GWASs) was investigated. A GWAS network was constructed by linking genes with the same phenotype from a database of GWAS results.[10] The overlap of the essential RH-PCR and CRISPRi networks with the GWAS network was then examined (**Figure 5A**).

The essential RH-PCR network showed significant overlap with the GWAS network (optimum FDR = 1.9×10^{-14}, OR = 2.0). The buffering, synergistic and combined K562 and Jurkat CRISPRi networks did not show significant overlap.

The significance of overlap between RH-PCR and the GWAS networks was greater using the entire RH-PCR network (optimum FDR = 7.2×10^{-319}, OR = 1.7), or a pruned network consisting of essential genes and genes separated by one link (optimum FDR = 4.5×10^{-250}, OR = 16.1) (**Figure 5B**).

The enhanced overlap of the RH-PCR and GWAS networks may reflect the less severe effect of an extra copy in the RH cells compared to the loss-of-function CRISPRi alleles. Most common alleles for GWAS loci are in transcriptional regulatory elements and have weaker effects than null alleles.[11]

The overlap of the RH-PCR and GWAS networks prompted an examination of whether loci from a higher powered GWAS could be predicted from a lower powered GWAS using the RH-PCR network.

Two GWASs of colorectal cancer were employed. The earlier and smaller GWAS had ∼35 000 cases and ∼71 000 controls and identified 70 loci.[12] The later GWAS with greater power had ∼100 000 cases and ∼155 000 controls, identifying 162 loci.[13] A total of 55 loci were shared between the two studies.

Interactions in the RH-PCR network that linked genes in the smaller study with genes in the larger study by a single step were significantly enriched compared to background (OR = 1.5, $P = 6.2 \times 10^{-6}$). Of the 107 genes for colorectal cancer found in the larger but not the smaller study, 40 were linked by the RH-PCR network to the smaller study (**Figure 5C**).

Examples of genes in the larger study linked by the RH-PCR network to those in the smaller study included genes with a role in oncogenic proliferation, such as *PDGFB* (linked to *HHIP* in the smaller study), *VAV2* (linked to 7 genes in the smaller study, including *BMP4*, *LAMC1*, *POLD3*) and *PTPRR* (*COL4A2*, *PREX1*, *SMAD6*).

In another example, two GWASs of height were evaluated. The higher powered study examined 5.4 million individuals and identified 2483 loci, while the lower

powered study examined ∼628 000 individuals and identified 893 loci.[14,15] A total of 529 loci were shared between the two studies.

There was significant enrichment of interactions in the RH-PCR network linking genes in the smaller study to genes in the larger (OR = 1.8, $P = 2.2 \times 10^{-308}$). Of the 1954 genes specific to the more highly powered study, 895 were linked by the RH-PCR network to genes in the lower powered study (**Figure 5D**).

The RH-PCR network may thus guide the search for additional candidate genes using data from modestly powered GWASs. Examples include GWASs of less common or expensive to ascertain phenotypes.

Discussion

Comparing the RH-PCR and the CRISPRi genetic interaction maps revealed the complementary properties of networks mediated by extra gene copies and partial loss-of-function, respectively.

The relatively non-toxic effects of increased gene copy number in the RH approach allows mapping of interactions for all genes and is reflected in the fact that retention of donor DNA is uniform across the entire genome.[1,4,7,16–19]

In contrast, the essential genes in the CRISPRi study were chosen for their moderate growth phenotype. The selection was necessary because interactions are difficult to assess when loss of one gene partner abolishes cell growth. Further, the relatively low throughput of the CRISPRi approach makes an evaluation of all interactions prohibitive.

The restriction of the CRISPRi network to genes with mild growth effects may introduce selection bias, even though comparisons included those in which the RH-PCR network was downsampled to the same genes as the CRISPRi network. Further differences between the interaction networks may emerge with higher extra copy numbers or stronger loss-of-function alleles.

Both the CRISPRi and RH-PCR maps showed significant overlap with the STRING database of protein-protein interactions. However, the CRISPRi interaction map showed greater overlap than the RH-PCR network restricted to essential genes. For the whole genome, the RH-PCR network showed superior overlap, probably because of its much larger size.

There was no significant overlap between the RH-PCR and CRISPRi interaction netowrks, reflecting their different mechanisms. This finding is consistent with a study showing that individual growth genes identified by partial inactivation using CRISPRi were different from those identified by overexpression using CRISPR activation (CRISPRa).[20]

However, the CRISPRi and RH-PCR networks showed significant overlap when analyzing the genes involved rather than the interactions. This observation suggests that partial loss-of-function and extra gene copies implicate similar genes in a biological process, but highlight different interaction partners.

Consistent with the foregoing conclusions, the essential RH-PCR network showed similar functional enrichments to that found in the CRISPRi network. GO analysis highlighted mitochondria and nucleus, while compartment clustering emphasized nucleus, cytoplasm and mitochondria, in that order. Other compartment classifications, such as early trafficking and cytoskeleton were not present in the RH-PCR network.

The complete RH-PCR network showed significant overlap with a network constructed from human GWAS data. In contrast, the CRISPRi network showed no overlap. The lack of overlap was not due to insufficient power, since an RH-PCR network constructed from the same genes as the CRISPRi network did show significant overlap with the GWAS network.

The significant overlap of the RH-PCR and the GWAS networks may reflect the fact that significant variants identified in GWAS tend to be located in transcriptional regulatory elements and affect RNA levels rather than protein sequence. The extra gene copies used in the RH-PCR network may thus be more similar to common GWAS variants than the partial loss-of-function alleles used in CRISPRi.

The overlap of the RH-PCR and GWAS networks is reminiscent of the finding that growth genes identified using bulk segregant analysis of RH cells showed significant overlap with GWAS genes, while growth genes identified using CRISPR did not.[17]

The RH approach relies on natural gene promoters to exert cellular effects. Similarly, CRISPRi will only result in a phenotype if the targeted gene is normally transcriptionally active.

In contrast, CRISPRa constitutively induces gene transcription using a catalytically dead version of Cas9 fused to a transcriptional activation domain.[20] This strategy results in uncontrolled overexpression. The RH and CRISPRi approaches therefore provide more physiologically relevant genotype/phenotype information than CRISPRa.

Materials and Methods

Data analysis

Statistical analyses used R.[21] Graphs were plotted using `ggplot2` and `cowplot`.[22,23] Networks were plotted using `Cytoscape` in the R environment implemented using `RCy3`.[24,25]

CRISPRi network

Buffering or synergistic CRISPRi interactions were classified as significant if the genetic interaction (GI) score was greater or less than the 95% confidence intervals of the negative controls, respectively.

For K562 cells, the GI threshold was 2.5 for buffering interactions and −2.6 for synergistic. For Jurkat cells, the thresholds were 1.9 and −2.0, respectively. Combined CRISPRi interactions were thresholded on GI score regardless of sign, with thresholds of 2.6 for K562 and 2.0 for Jurkat.

Clustering of RH-PCR network

Clustering of the RH-PCR interactions for essential genes used `heatmap.2` with Euclidean distance measures.[26] Clusters were defined using dendrogram cuts closest to origin. Genes were assigned to GO categories using `ontologyIndex`.[27] Significance values for GO enrichment of clusters were calculated using Fisher's Exact Test.

Assignment of cell compartments for interacting pairs of essential genes in the RH-PCR network was performed as described.[5]

GWAS network

The GWAS network was constructed by linking all genes associated with the same phenotype. The $-\log_{10} P$ for the interactions was calculated as the mean value for each trait.

Overlap comparisons of the essential RH-PCR and GWAS networks employed the full GWAS network. However, comparisons of the essential RH-PCR plus one and the full protein coding RH-PCR networks used the GWAS network downsampled 20-fold to allow manageable computation times.

Data availability

All analyzed data is publicly available as described in the relevant citations. The data, together with the code used for analysis, is also available from figshare (https://figshare.com/; doi: 10.6084/m9.figshare.25148660).

Author contributions

DJS: conceptualization, methodology, software, formal analysis, investigation, data curation, writing – original draft, writing – review and editing, visualization.

Conflict of Interest

The author declares no conflict of interest.

Acknowledgments

I thank Jake Lusis for helpful comments on the manuscript.

Supporting information is available.

References

1. Khan, A.H. and Smith, D.J. (2021). Cost-effective mapping of genetic interactions in mammalian cells. Front. Genet. *12*, 703738. https://doi.org/10.3389/fgene.2021.703738.

2. Goss, S.J. and Harris, H. (1975). New method for mapping genes in human chromosomes. Nature *255*, 680–684. https://doi.org/10.1038/255680a0.

3. Cox, D.R., Burmeister, M., Price, E.R., Kim, S., and Myers, R.M. (1990). Radiation hybrid mapping: a somatic cell genetic method for constructing high-resolution maps of mammalian chromosomes. Science *250*, 245–250. https://doi.org/10.1126/science.2218528.

4. Lin, A., Wang, R.T., Ahn, S., Park, C.C., and Smith, D.J. (2010). A genome-wide map of human genetic interactions inferred from radiation hybrid genotypes. Genome Res. *20*, 1122–1132. https://doi.org/10.1101/gr.104216.109.

5. Horlbeck, M.A., Xu, A., Wang, M., Bennett, N.K., Park, C.Y., Bogdanoff, D., Adamson, B., Chow, E.D., Kampmann, M., Peterson, T.R., et al. (2018). Mapping the genetic landscape of human cells. Cell *174*, 953–967.e22. https://doi.org/10.1016/j.cell.2018.06.010.

6. Benjamini, Y. and Hochberg, Y. (1995). Controlling the false discovery rate: a practical and powerful approach to multiple testing. J. Royal Stat. Soc. Series B-Methodological, 289–300. https://doi.org/10.1111/j.2517-6161.1995.tb02031.x.

7. Ahn, S., Wang, R.T., Park, C.C., Lin, A., Leahy, R.M., Lange, K., and Smith, D.J. (2009). Directed mammalian gene regulatory networks using expression and comparative genomic hybridization microarray data from radiation hybrids. PLoS Comput Biol. *5*, e1000407. https://doi.org/10.1371/journal.pcbi.1000407.

8. Szklarczyk, D., Gable, A.L., Lyon, D., Junge, A., Wyder, S., Huerta-Cepas, J., Simonovic, M., Doncheva, N.T., Morris, J.H., Bork, P., et al. (2019). STRING v11: protein-protein association networks with increased coverage, supporting functional discovery in genome-wide experimental datasets. Nucleic Acids Res *47*, D607–D613. https://doi.org/10.1093/nar/gky1131.

9. Gene Ontology Consortium, Aleksander, S.A., Balhoff, J., Carbon, S., Cherry, J.M., Drabkin, H.J., Ebert, D., Feuermann, M., Gaudet, P., Harris, N.L.,

et al. (2023). The Gene Ontology knowledgebase in 2023. Genetics *224*, iyad031. https://doi.org/10.1093/genetics/iyad031.

10. Sollis, E., Mosaku, A., Abid, A., Buniello, A., Cerezo, M., Gil, L., Groza, T., Güneş, O., Hall, P., Hayhurst, J., et al. (2023). The NHGRI-EBI GWAS Catalog: knowledgebase and deposition resource. Nucleic Acids Res. *51*, D977–D985. https://doi.org/10.1093/nar/gkac1010.

11. Nasser, J., Bergman, D.T., Fulco, C.P., Guckelberger, P., Doughty, B.R., Patwardhan, T.A., Jones, T.R., Nguyen, T.H., Ulirsch, J.C., Lekschas, F., et al. (2021). Genome-wide enhancer maps link risk variants to disease genes. Nature *593*, 238–243. https://doi.org/10.1038/s41586-021-03446-x.

12. Law, P.J., Timofeeva, M., Fernandez-Rozadilla, C., Broderick, P., Studd, J., Fernandez-Tajes, J., Farrington, S., Svinti, V., Palles, C., Orlando, G., et al. (2019). Association analyses identify 31 new risk loci for colorectal cancer susceptibility. Nat. Commun. *10*, 2154. https://doi.org/10.1038/s41467-019-09775-w.

13. Fernandez-Rozadilla, C., Timofeeva, M., Chen, Z., Law, P., Thomas, M., Schmit, S., Díez-Obrero, V., Hsu, L., Fernandez-Tajes, J., Palles, C., et al. (2023). Deciphering colorectal cancer genetics through multi-omic analysis of 100,204 cases and 154,587 controls of European and east Asian ancestries. Nat. Genet. *55*, 89–99. https://doi.org/10.1038/s41588-022-01222-9.

14. Sakaue, S., Kanai, M., Tanigawa, Y., Karjalainen, J., Kurki, M., Koshiba, S., Narita, A., Konuma, T., Yamamoto, K., Akiyama, M., et al. (2021). A cross-population atlas of genetic associations for 220 human phenotypes. Nat Genet *53*, 1415–1424. https://doi.org/10.1038/s41588-021-00931-x.

15. Yengo, L., Vedantam, S., Marouli, E., Sidorenko, J., Bartell, E., Sakaue, S., Graff, M., Eliasen, A.U., Jiang, Y., Raghavan, S., et al. (2022). A saturated map of common genetic variants associated with human height. Nature *610*, 704–712. https://doi.org/10.1038/s41586-022-05275-y.

16. Khan, A.H., Bloom, J.S., Faridmoayer, E., and Smith, D.J. (2016). Genetic screening reveals a link between Wnt signaling and antitubulin drugs. Pharmacogenomics J. *16*, 164–172. https://doi.org/10.1038/tpj.2015.50.

17. Khan, A.H., Lin, A., Wang, R.T., Bloom, J.S., Lange, K., and Smith, D.J. (2020). Pooled analysis of radiation hybrids identifies loci for growth and drug action in mammalian cells. Genome Res. *30*, 1458–1467. https://doi.org/10.1101/gr.262204.120.

18. Lin, A. and Smith, D.J. (2015). Copy number networks to guide combinatorial therapy of cancer and proliferative disorders. In Emerging Trends in Computational Biology, Bioinformatics, and Systems Biology - Algorithms and Software Tools, Q.-N. Tran and H.R. Arabnia, eds. (Elsevier Morgan Kaufmann), pp. 401–419.

19. Wang, R.T., Ahn, S., Park, C.C., Khan, A.H., Lange, K., and Smith, D.J. (2011). Effects of genome-wide copy number variation on expression in mammalian cells. BMC Genomics *12*, 562. https://doi.org/10.1186/1471-2164-12-562.

20. Gilbert, L.A., Horlbeck, M.A., Adamson, B., Villalta, J.E., Chen, Y., Whitehead, E.H., Guimaraes, C., Panning, B., Ploegh, H.L., Bassik, M.C., et al. (2014). Genome-scale CRISPR-mediated control of gene repression and activation. Cell *159*, 647–661. https://doi.org/10.1016/j.cell.2014.09.029.

21. R Core Team (2023). R: A language and environment for statistical computing. (Vienna, Austria). https://www.R-project.org/.

22. Wickham, H. (2016). `ggplot2`: Elegant Graphics for Data Analysis (Springer-Verlag New York). https://ggplot2.tidyverse.org.

23. Wilke, C.O. (2020). `cowplot`: Streamlined Plot Theme and Plot Annotations for 'ggplot2'. R package version 1.1.1. https://CRAN.R-project.org/package=cowplot.

24. Gustavsen, A., J., Pai, Shraddha, Isserlin, Ruth, Demchak, Barry, Pico, and R., A. (2019). `RCy3`: Network biology using Cytoscape from within R. F1000Research. https://doi.org/10.12688/f1000research.20887.3.

25. Shannon, P., Markiel, A., Ozier, O., Baliga, N.S., Wang, J.T., Ramage, D., Amin, N., Schwikowski, B., and Ideker, T. (2003). `Cytoscape`: a software environment for integrated models of biomolecular interaction networks. Genome Res. *13*, 2498–2504. https://doi.org/10.1101/gr.1239303.

26. Warnes, G.R., Bolker, B., Bonebakker, L., Gentleman, R., Huber, W., Liaw, A., Lumley, T., Maechler, M., Magnusson, A., Moeller, S., et al. (2022). `gplots`: Various R programming tools for plotting

data. R package version 3.1.3. https://CRAN.R-project.org/package=gplots.

27. Greene, D., Richardson, S., and Turro, E. (2017). ontologyX: a suite of R packages for working with ontological data. Bioinformatics *33*, 1104–1106. https://doi.org/10.1093/bioinformatics/btw763.

Supplemental Information: Complementary human gene interaction maps from radiation hybrids and CRISPRi

Desmond J. Smith[1,*]

[1] *Department of Molecular and Medical Pharmacology, David Geffen School of Medicine, UCLA, Los Angeles, USA*
[*] *DSmith@mednet.ucla.edu*

Supplemental Figures

S1 CRISPRi and STRING networks in K562 cells s2
S2 CRISPRi and STRING networks in Jurkat cells s3
S3 RH-PCR, CRISPRi and STRING networks s4
S4 Genes in RH-PCR and K562 CRISPRi networks s5
S5 Overlap of genes in RH-PCR and Jurkat CRISPRi networks s6
S6 Genes in RH-PCR and Jurkat CRISPRi networks s7

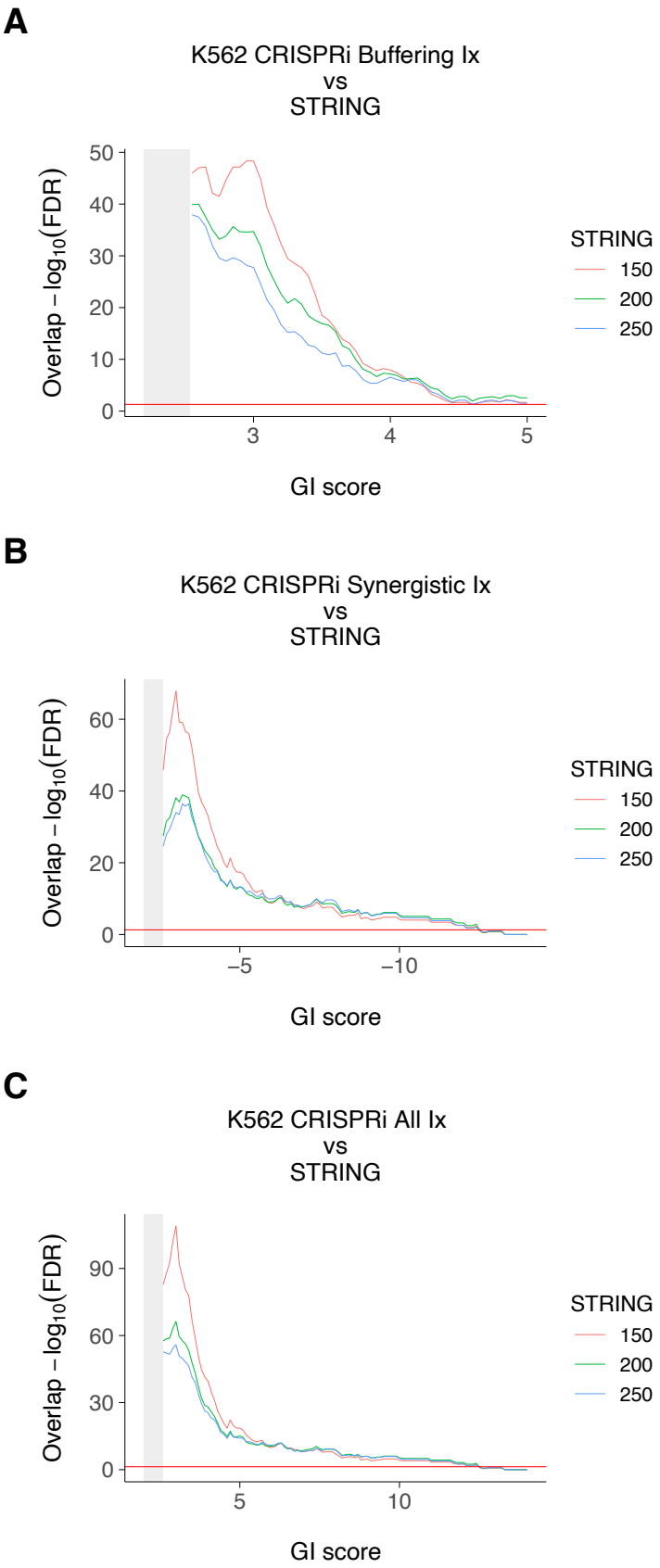

Figure S1. CRISPRi and STRING networks in K562 cells. (**A**) Overlap of K562 buffering CRISPRi interactions and STRING. (**B**) Overlap of K562 synergistic CRISPRi interactions and STRING. (**C**) Overlap of K562 combined buffering and synergistic CRISPRi interactions and STRING. Gray areas indicate insignificant CRISPRi genetic interaction (GI) scores.

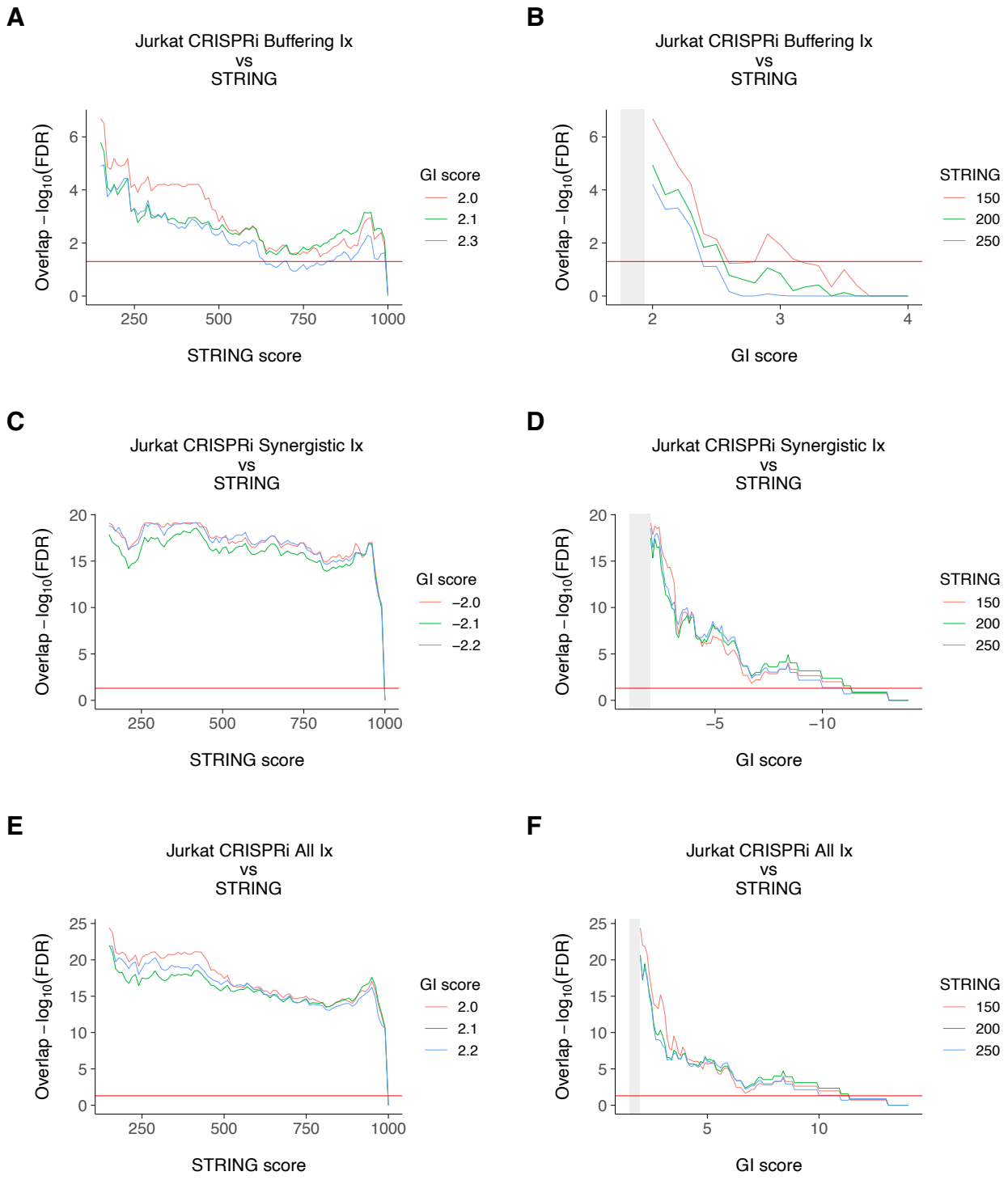

Figure S2. CRISPRi and STRING networks in Jurkat cells. (**A**,**B**) Overlap of Jurkat buffering CRISPRi interactions and STRING. (**C**,**D**) Overlap of Jurkat synergistic CRISPRi interactions and STRING. (**E**,**F**) Overlap of Jurkat combined buffering and synergistic CRISPRi interactions and STRING. Gray areas indicate insignificant CRISPRi GI scores.

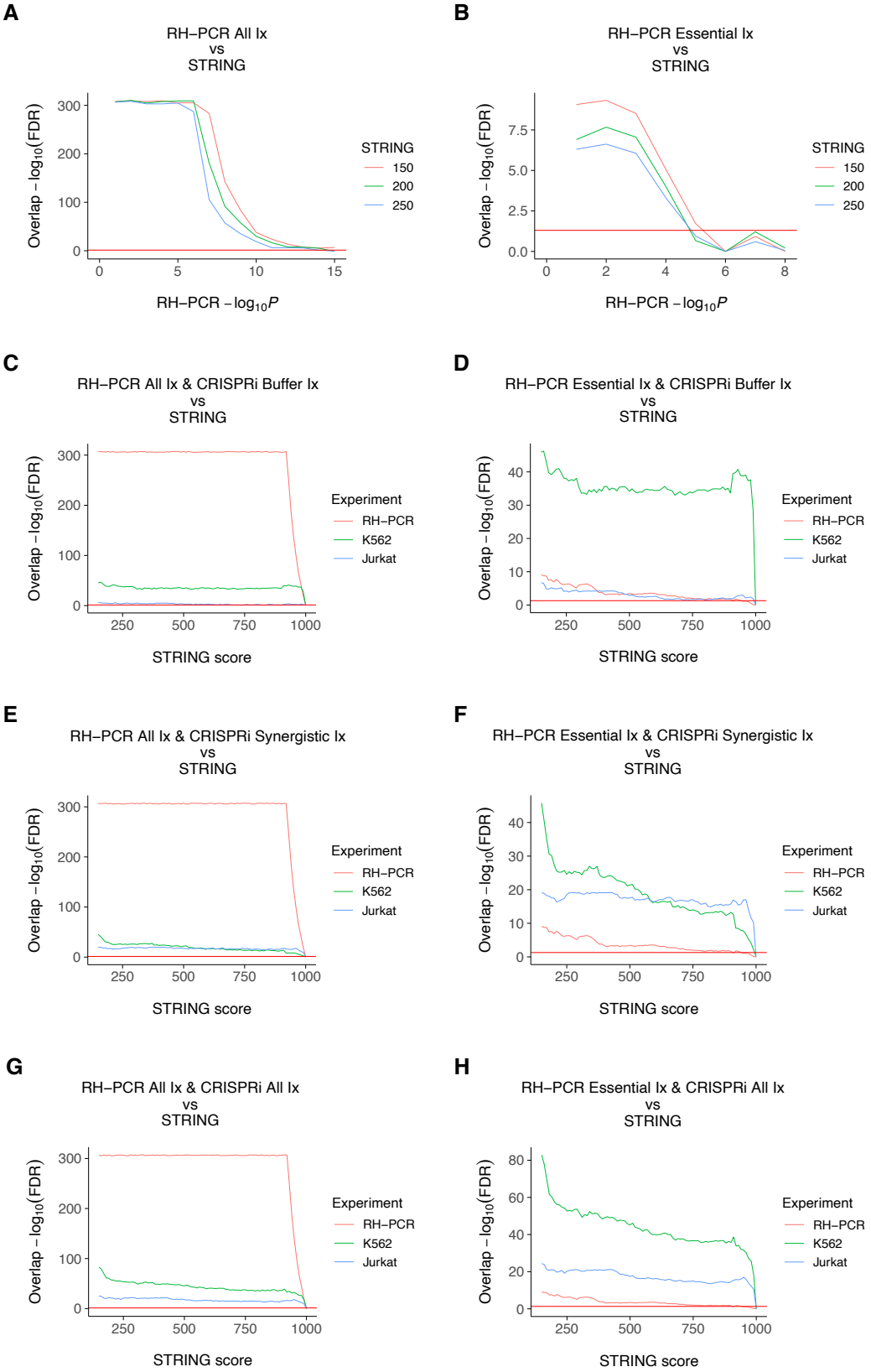

Figure S3. Overlaps of RH-PCR, CRISPRi and STRING networks. (**A**) Overlap of protein coding RH-PCR network and STRING. (**B**) Overlap of RH-PCR interactions restricted to CRISPRi essential genes and STRING. (**C**) Overlap of protein coding RH-PCR, buffering CRISPRi, and STRING networks. (**D**) Overlap of essential RH-PCR, buffering CRISPRi, and STRING networks. (**E**) Overlap of protein coding RH-PCR, synergistic CRISPRi, and STRING networks. (**F**) Overlap of essential RH-PCR, synergistic CRISPRi, and STRING networks. (**G**) Overlap of protein coding RH-PCR, combined buffering and synergistic CRISPRi, and STRING networks. (**H**) Overlap of essential RH-PCR, combined CRISPRi, and STRING networks.

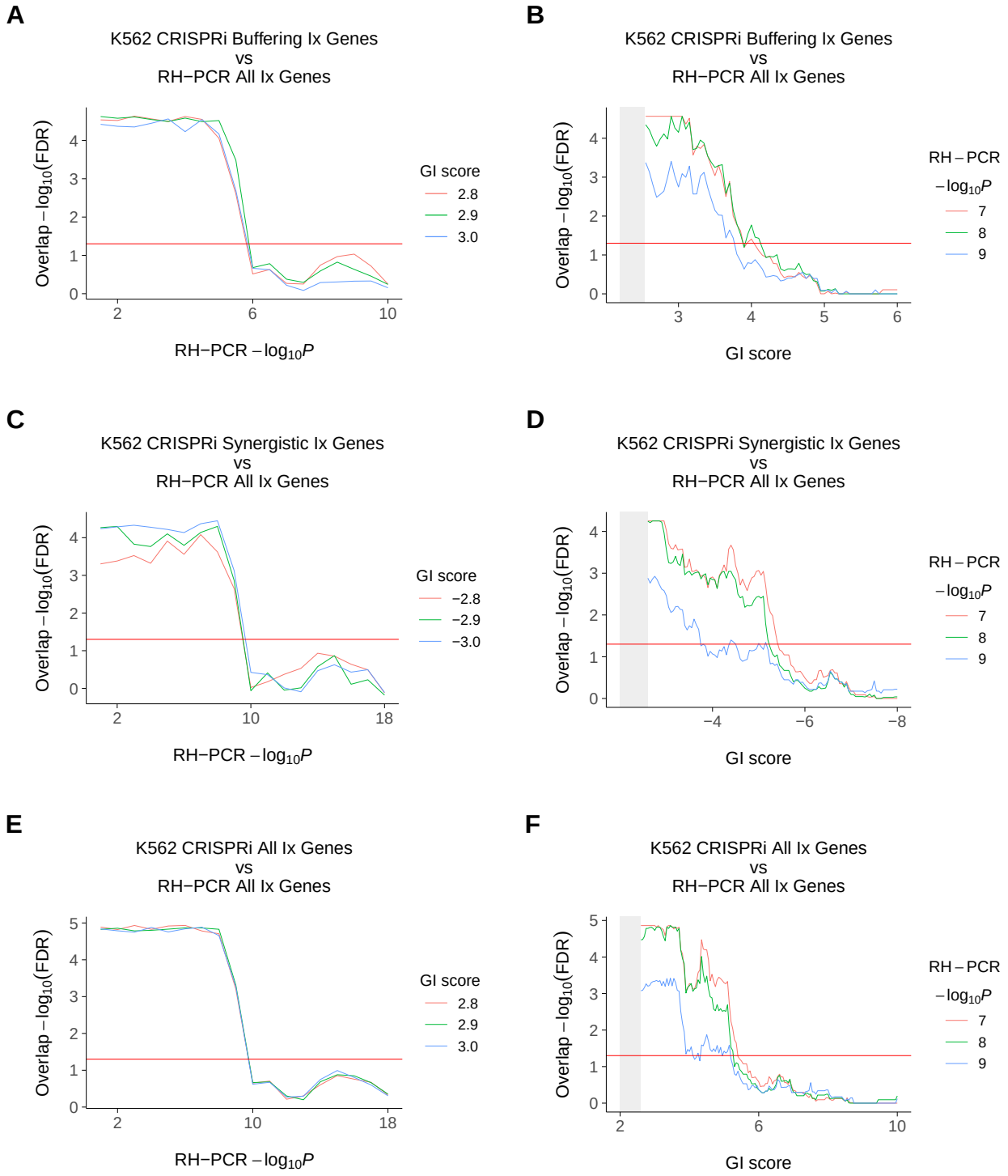

Figure S4. Genes in RH-PCR and K562 CRISPRi networks. (**A**, **B**) Overlap of genes in K562 buffering CRISPRi and protein coding RH-PCR networks. (**C**,**D**) Overlap of genes in K562 synergistic CRISPRi and protein coding RH-PCR networks. (**E**, **F**) Overlap of genes in K562 combined buffering and synergistic CRISPRi and protein coding RH-PCR networks.

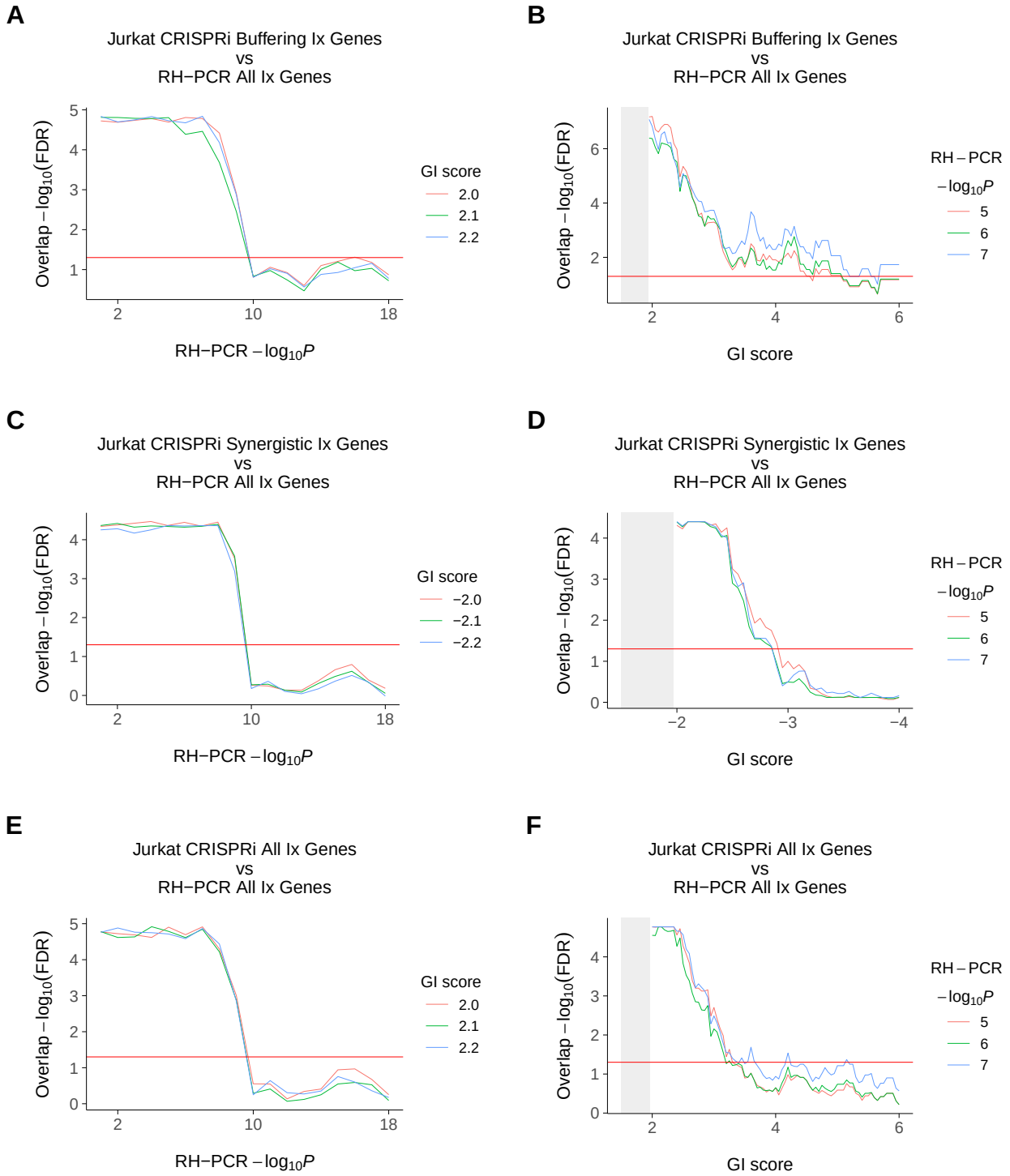

Figure S5. Genes in RH-PCR and Jurkat CRISPRi networks. (**A**, **B**) Overlap of genes in Jurkat buffering CRISPRi and protein coding RH-PCR networks. (**C**,**D**) Overlap of genes in Jurkat synergistic CRISPRi and protein coding RH-PCR networks. (**E**, **F**) Overlap of genes in Jurkat combined buffering and synergistic CRISPRi and protein coding RH-PCR networks.

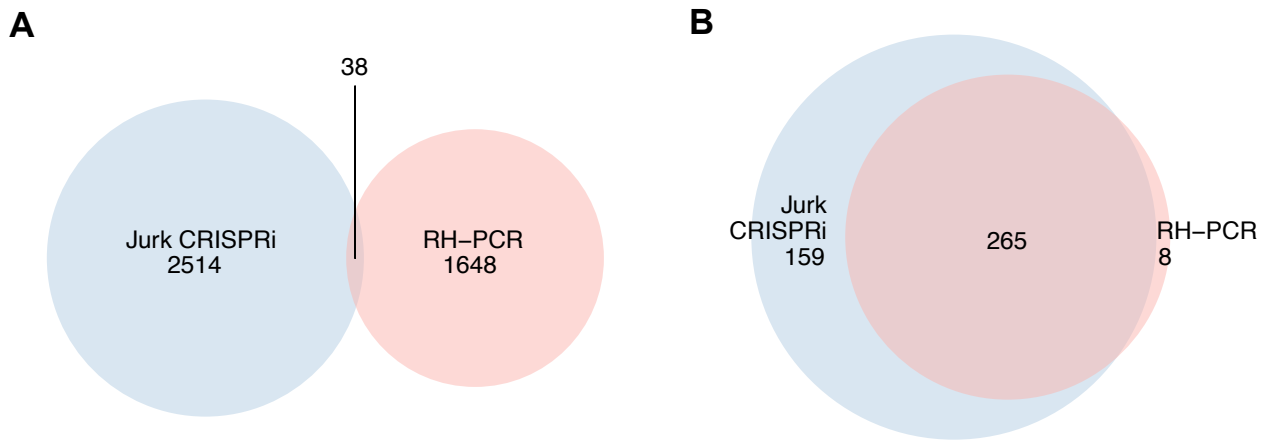

Figure S6. Genes in RH-PCR and Jurkat CRISPRi networks. (**A**) Overlap of interactions in the essential RH-PCR and Jurkat combined buffering and synergistic CRISPRi networks. (**B**) Overlap of genes involved in interactions in the two networks.